Published in final edited form as:

Environ Sci Technol Lett. 2023 ; 10(8): . doi:10.1021/acs.estlett.3c00318.

Ozone Generation from a Germicidal Ultraviolet Lamp with Peak Emission at 222 nm

Michael F. Link[1,*], **Andrew Shore**[1], **Behrang H. Hamadani**[1], **Dustin Poppendieck**[1,*]

[1]National Institute of Standards and Technology, Gaithersburg, MD, 20899, USA

Abstract

Recent interest in commercial devices containing germicidal ultraviolet lamps with a peak emission wavelength at 222 nm (GUV222) has focused on mitigating virus transmission indoors while posing minimum risk to human tissue. However, 222 nm light can produce ozone (O_3) in air. O_3 is an undesirable component of indoor air because of health impacts from acute to chronic exposure and its ability to degrade indoor air quality through oxidation chemistry. In seven four-hour experiments we measured O_3 produced from a single filtered GUV222 lamp in a 31.5 m^3 stainless steel chamber. Using an emission model, we determined an O_3 generation rate of 19.4 $ppb_v\ h^{-1}$ ± 0.3 $ppb_v\ h^{-1}$ (equivalent to 1.22 mg h^{-1} ± 0.02 mg h^{-1}). We estimated the fluence rate from the lamp using two methods: (1) chemical actinometry using tetrachloroethylene (actinometry) and (2) geometric projection of the irradiance field from radial and angular distribution measurements of the GUV222 lamp fluence (irradiance). Using the estimated lamp fluence rates of 2.2 μW cm^{-2} (actinometry) and 3.2 μW cm^{-2} (irradiance) we predicted O_3 production in our chamber within 20 % of the average measured mixing ratio. Future studies should evaluate the indoor air quality impacts of GUV222 technologies.

Keywords

air cleaning; germicidal ultraviolet light; ozone; indoor air quality

Introduction

The on-going COVID-19 pandemic has highlighted the need for effective, in room, low energy air cleaning devices to enable safer in-person interactions in indoor environments.[1,2,3] Portable cleaning devices use a range of technologies that have uncharacterized impacts on indoor air quality.[4] These impacts could result in human exposure to pollutants that are at odds with the intended benefit of the technology.[5] One such technology is germicidal ultraviolet lamps that operate with a peak emission wavelength at 222 nm (GUV222). This wavelength is appealing as research to date indicates it does not significantly penetrate human skin and is effective at inactivating pathogens.[6,7,8]

[*] *Corresponding authors:* michael.f.link@nist.gov; dustin.poppendieck@nist.gov.

Supporting Information

Details on the irradiance projection calculation, actinometry, ozone decay examples, and a brief comparison of ozone generation results to recent studies.

Air cleaning devices equipped with GUV222 are of particular importance when considering the potential for ozone (O_3) formation. In the range of 175 nm to 242 nm, molecular oxygen (O_2) will absorb light and dissociate with a quantum yield of unity to produce two ground state oxygen atoms (O; Reaction 1) that can then go on to recombine with O_2, in a termolecular reaction involving a collisional body (M = N_2 or O_2), to form O_3 via Reaction 2.[9, 10,11]

$$O_2 + h\upsilon\ (\lambda = 175\ nm\ to\ 242\ nm) \rightarrow 2\ O \quad \text{(R1)}$$

$$O + O_2 + M \rightarrow O_3 + M \quad \text{(R2)}$$

Reactions 1 and 2 are known to occur in the stratosphere where deep UV radiation is available.[12] Characterization of spectral output and potential for O_3 production is necessary when considering the application of GUV222 devices for mitigating virus transmission while maintaining good air quality in indoor environments.

While O_3 itself can be a harmful byproduct of air cleaner operation[13], it can also react with gases and surfaces indoors[14]—including human skin[15]—leading to the formation of other potentially concerning byproducts such as gas-phase aldehydes and ultra-fine particulate matter[16]. Of particular concern is the exposure to O_3 and O_3-generated indoor pollutant byproducts from application of multiple GUV222 units in small and/or poorly ventilated indoor spaces.[17] Here we present measurements of O_3 generation from a commercial GUV222 lamp in a stainless steel laboratory chamber, support our O_3 formation observations with a chemical kinetic model, and determine O_3 generation rates for this GUV222 lamp that can be used in future evaluations of GUV222 technologies in indoor spaces.

Methods

Measurement of the GUV222 Lamp Emission Spectrum.

Spectral irradiance measurements of a krypton chloride (KrCl) excimer GUV222 lamp were performed with a commercial UV spectrometer with detection sensitivity in the spectral range of 200 nm to 415 nm. GUV222 emission light was collected by an integrating sphere detector that was connected to the spectrometer by a UV-transmitting optical fiber patch cable. We estimate the uncertainty (k=2) of the spectral irradiance measurements at 222 nm to be 18 %. Additional details are provided in the supplemental information.

Operation of Chamber and Experiment Design.

We operated the commercial GUV222 lamp in a 31.5 m^3 environmentally controlled walk-in chamber instrumented to measure O_3 and sulfur hexafluoride (SF_6; proton-transfer mass spectrometry) which was used to measure the chamber air change rate (Figure S8). A series of seven experiments were conducted to measure O_3 production from the GUV222 lamp. A

metal fan was placed in the chamber to facilitate mixing. The GUV222 lamp was positioned in the upper corner of the chamber pointed down and towards the center of the chamber opposite of the fan (Figure S4). Two days prior to the seven GUV222 experiments the chamber was sealed and passivated with at least 100 ppb_v of O_3 for a total of 24 hours.

Prior to each experiment we operated the chamber to achieve a temperature of 20 °C and 50 % relative humidity. The chamber maintained a pressure of 101 kPa. Low levels of O_3, particulate matter, and volatile organic compound contaminants were achieved by passing outdoor air through MERV-13, carbon, and chemisorbant filters. This filtered outdoor air was recirculated in the chamber prior to each experiment. At the beginning of each experiment the chamber was sealed. The GUV222 lamp was then turned on for four hours over which O_3 concentration was measured. SF_6 was injected into the chamber at the start of each experiment and air change was determined from the first order loss constant (Figure S8). Tetrachloroethylene (C_2Cl_4) was vaporized and introduced to the chamber at the beginning of four of the experiments to measure the effective photon flux via actinometry (e.g., Peng, et al. 2023)[18].

Results and Discussion

GUV222 Lamp Emission Spectrum.

Figure 1a shows the spectral irradiance versus wavelength of the GUV222 lamp measured directly under and at several distances from the lamp.

The main emission peak is at 222 nm, as reported by other studies examining emission spectra of KrCl lamps.[19,20] The lamp used in this study was a “filtered” lamp that the manufacturer states filters radiation from the emission band around 190 nm. We determined the total irradiance by integrating under the spectral irradiance curve over the entire emission range (Figure 1b). The total irradiance in the immediate vicinity of the lamp is high (105 W m^{-2} at 0 cm and 27 W m^{-2} at 5 cm) but drops very quickly with distance. The drop-off in total irradiance follows the relationship, $E \sim 1/d^{1.52}$, at least up to 40 cm where E is irradiance and d the distance from the lamp. We find that the irradiance projection from the lamp is attenuated by 50 % at a projection angle of 35 ° and becomes negligible at an angle of 55 ° (Figure 1c).

Measurement and Modeling of O_3 Production from GUV222.

We measured elevated levels of O_3 in our chamber after four hours of GUV222 operation as shown in Figure 2.

Four hours after turning the GUV222 lamp on, we observed 53 $ppb_v \pm 1$ ppb_v (106 μg $m^{-3} \pm 2$ μg m^{-3}) of O_3 in the chamber. To rule out the influence of other physical phenomena related to operation of the GUV222 lamp (e.g., electrical arching[13]) that could be responsible for O_3 production we operated the lamp, for one experiment, with the output covered to prevent light from illuminating the chamber. No O_3 generation was observed in that experiment (Figure 2, purple trace) providing evidence that photolysis of O_2 at 222 nm was responsible for production of O_3.

At the end of each experiment the lamp was turned off and the decay of O_3 was measured (Figure S6). We assume that O_3 is lost to stainless steel chamber surfaces and homogeneous gas-phase reactions via a first order process (k_{loss}). Additionally, some O_3 is lost via air change which was quantified from SF_6 decay measurements (e.g., removal via air change accounts for ≈ 6 % of total observed O loss; Figure S8). We determine the rate constant for the combined loss processes (k_{decay}) from a linear fit of the natural log of the O_3 mixing ratio versus time (Equation 1).

$$\ln\left(\frac{[O_3]_t}{[O_3]_0}\right) = -k_{decay}t = -(k_{\dot{V}} + k_{loss})t \quad \text{(Eqn. 1)}$$

In Equation 1, k_{loss} is the first order rate constant for loss of O_3 to the chamber surfaces and homogeneous gas-phase reactions, $k_{\dot{V}}$ is the air change rate (h^{-1}), and t is time. We determine k_{loss} by subtracting the $k_{\dot{V}}$ term (determined from decay measurements of SF_6) from the measured k_{decay}. The rate constants for O_3 decay (k_{decay}) remained constant throughout the experiments varying by 2 % (Table 1).

We calculate theoretical O_3 production from GUV222 using chemical production and loss and physical loss terms in Equation 2.

$$\frac{d[O_3]}{dt} = 2j_{O2}[O_2] - \frac{2k_1 jO_3[O_3]^2}{k_2[O_2][M]} - (k_{\dot{V}} + k_{decay})[O_3] \quad \text{(Eqn. 2)}$$

The first term on the right hand side of Equation 2 is the O_3 production from photolysis of O_2 at 222 nm, the second term accounts for loss of O_3 through the odd-oxygen ($O_x = O_3 + O$) steady-state ($k_1 = 7.96 \times 10^{-15}$ cm^3 molecule^{-1} s^{-1}; $k_2 = 6.10 \times 10^{-34}$ cm^6 molecule^{-2} s^{-1}) where [M] is the number density of air (M = N_2, O_2), and the third term accounts for depositional loss to chamber walls and homogeneous gas-phase reactions.

As shown in Equation 2, the photolysis rate of O_2 drives O_3 production from GUV222 and the first-order photolysis rate constant (j_{O2}) is strongly dependent on the photon flux (F; Equation 3) from the lamp.

$$j_{O2} = \int \sigma_{O2}\Phi_{O2}F\, d\lambda \quad \text{(Eqn. 3)}$$

Using the measured irradiance spectrum (Figure 1a) from the lamp we calculate an effective O_2 absorption cross section (σ_{O2})[9] of 4.30×10^{-24} cm^2 across a wavelength (λ) range between 210 nm and 230 nm (compared to 4.09×10^{-24} cm^2 at 222 nm). The photolysis quantum yield of O_2 (Φ_{O2}) between 210 nm and 230 nm is unity.[21] We estimate an effective

photon flux (F) from GUV222 from two different methods: (1) by determining the average of the measured irradiance projected into a cone (irradiance method) and (2) following the method of Peng, et al. (2023)[18], using chemical actinometry[22] with C_2Cl_4 as the actinometer (actinometry method).

For the irradiance method, we generated an irradiance field within a 31.5 m^3 cone by expanding the GUV222 irradiance point source axially following the relationship, $E \sim 1/d^{1.52}$, and angularly following a relatively tight half-angle of ≈ 55° (Equation S4). We then averaged the projected irradiance over the emission volume to get the effective photon flux. For the actinometry method, C_2Cl_4 was introduced to the chamber and the GUV222 lamp was turned on for four hours to measure the C_2Cl_4 photolysis rate. Using the measured C_2Cl_4 photolysis rate, effective C_2Cl_4 absorption cross section (σ_{C2Cl4})[23], and reported photolysis quantum yield (Φ_{C2Cl4}), we determined the effective photon flux (Equation S8). Between 210 nm and 230 nm, effective GUV222 fluence rates of 3.2 μW cm^{-2} and 2.2 μW cm^{-2} were determined from the irradiance method and actinometry, respectively. Using our average measured O_3 from the experiments and solving for the photon flux through our chemical model, we estimate an experimentally determined effective fluence rate of the GUV222 lamp to be 2.6 μW cm^{-2}. Details of the effective photon flux determination methods are discussed in the supplemental information.

For the irradiance method, O_3 levels are over-predicted by 18 %. We expect over-estimation of the effective photon flux using this irradiance method because we are not accounting for attenuation of the incident radiation by interactions with the chamber walls. Ma, et al. (2023) recently demonstrated that different types of stainless steel reflect 222 nm light with an efficiency on the order of 20 %.[24] The 31.5 m^3 modeled conical irradiance field slightly extends beyond the chamber walls, but the lamp was positioned in a corner of the chamber such that a large volume of the chamber air was irradiated by the UV light. Our calculations indicate most of the O_3 is created within 2 m of the lamp (Table S1), so the cone extending beyond the chamber walls results in small overestimation of O_3 production. Accurately accounting for reflectance and exact chamber dimensions would decrease the effective photon flux and thus modeled O_3 production.

In contrast to the irradiance method, the model underpredicts O_3 levels by 18 % using the actinometry method. An effective fluence rate of 2.6 μW cm^{-2} (k_{decay}= 0.19 h^{-1}) would be needed to reconcile the 18 % deficit in modeled O_3 production. Despite some discrepancies between modeled and measured O_3, our calculations provide evidence to suggest the mechanism of O_3 production from our GUV222 lamp is photolysis of O_2 from 222 nm light, and not from other physical phenomena (e.g., electrical arching).

Determination of O_3 Generation Rates from GUV222 Lamps.

In the chamber experiments O_3 was generated from GUV222 while simultaneously being lost through air change, gas-phase reactions, and deposition to surfaces. Thus, the O_3 production rate from the lamp can be determined by solving for the generation rate (GR) in the transient solution to the mass balance equation presented in Equation 4.

$$[O_3]_t = [O_3]_i\, e^{-(k_{\dot{V}} + k_{decay})t} + \frac{\frac{GR}{V}}{(k_{\dot{V}} + k_{decay})(1 - e^{-(k_{\dot{V}} + k_{decay})t})}$$

(Eqn. 4)

Where $[O_3]_i$ and $[O_3]_t$ are the initial and time t O_3 mixing ratios, V is the volume of the chamber (31.5 m^3), and GR is the O_3 generation rate (μg h^{-1}).

Calculated GUV222 O_3 generation rates (converted from μg h^{-1} to ppb_v h^{-1} using the 31.5 m^3 chamber volume), presented in Table 1, varied within 2%.

From an average of seven experiments, we measured an O_3 generation rate from the GUV222 lamp of 19.4 ppb_v h^{-1} ± 0.3 ppb_v h^{-1} (equivalent to 1.22 mg h^{-1} ± 0.02 mg h^{-1}) that, from our chemical modeling, implies a lamp fluence rate of 2.6 μW cm^{-2}.

We measured the spectral irradiance of a commercial GUV222 lamp from 210 nm to 230 nm showing a peak emission at 222 nm. Results from seven replicate experiments of the single commercial GUV222 lamp used in this study yielded a mean O_3 generation rate of 19.4 ppb_v h^{-1} and, from our chemical modeling, implies a lamp fluence rate of 2.6 μW cm^{-2}. The results observed in this study apply to this lamp and may vary between unit, manufacturer, and test conditions. For instance, when comparing the GUV222 fluence rate normalized O_3 production rate (i.e., O_3 production rate/fluence rate = O_3 production efficiency) measured in this study to two other recent studies[18,25] we find that the O_3 production efficiencies can vary within 30 % when measured from the same model lamp (Table S2).

O_3 generation rates determined in this study could be used to predict O_3 production and accumulation in indoor spaces from commercial GUV222 lamps like the one used in this study. We note that the effective fluence rate (i.e., average amount of light irradiating a given volume; Table S2) will depend on the GUV222 path length and so the O_3 generation values reported here are most applicable to indoor spaces with volumes equal to, or larger than, 31.5 m^3. Like the losses of O_3 to chamber walls and gas-phase reactions we observed, much higher reactive losses of O_3 generated from GUV222 devices would be expected in real indoor environments (e.g., k_{loss} = 2 h^{-1} (surfaces) and k_{loss} = 0.09 h^{-1} per person (human envelope))[26] with potential impacts for byproduct formation that would affect indoor air quality[27]. Additionally, we note that the radiation dosing necessary to achieve high levels of virus deactivation may require multiple GUV222 lamps[28] and thus our measured O_3 generation rate could be used to simulate the effects of multiple lamp installations on indoor air quality. We suggest more measurements of O_3 production should be made from commercial air cleaning devices that use GUV222 lamps to assess the impacts on indoor air quality in both real indoor and laboratory settings.

Supplementary Material

Refer to Web version on PubMed Central for supplementary material.

Acknowledgments

We would like to acknowledge James Norris and Peter Trask for calibration of the ozone instrument used in this study. We would like to thank Howard Yoon and Cameron Miller for assistance with irradiance calibrations of our UV spectroradiometers. We thank and acknowledge Jose Jimenez for providing recommendations for experimental design.

References

(1). Guettari M; Gharbi I; Hamza S UVC disinfection robot. Environmental Science and Pollution Research 2021, 28, 40394–40399. [PubMed: 33058078]

(2). Mousavi ES; Kananizadeh N; Martinello RA; Sherman JD COVID-19 outbreak and hospital air quality: a systematic review of evidence on air filtration and recirculation. Environmental science & technology 2020, 55 (7), 4134–4147. [PubMed: 32845618]

(3). Lindsley WG; Derk RC; Coyle JP; Martin SB Jr; Mead KR; Blachere FM; Beezhold DH; Brooks JT; Boots T; Noti JD Efficacy of portable air cleaners and masking for reducing indoor exposure to simulated exhaled SARS-CoV-2 aerosols—United States, 2021. Morbidity and Mortality Weekly Report 2021, 70 (27), 972. [PubMed: 34237047]

(4). Collins DB; Farmer DK Unintended consequences of air cleaning chemistry. Environmental Science & Technology 2021, 55 (18), 12172–12179. [PubMed: 34464124]

(5). Cheek E; Guercio V; Shrubsole C; Dimitroulopoulou S Portable air purification: Review of impacts on indoor air quality and health. Science of the total environment 2021, 766, 142585. [PubMed: 33121763]

(6). Narita K; Asano K; Morimoto Y; Igarashi T; Nakane A Chronic irradiation with 222-nm UVC light induces neither DNA damage nor epidermal lesions in mouse skin, even at high doses. PloS one 2018, 13 (7), e0201259. [PubMed: 30044862]

(7). Buonanno M; Welch D; Shuryak I; Brenner DJ Far-UVC light (222 nm) efficiently and safely inactivates airborne human coronaviruses. Scientific Reports 2020, 10 (1), 1–8. [PubMed: 31913322]

(8). Ma B; Gundy PM; Gerba CP; Sobsey MD; Linden KG UV inactivation of SARS-CoV-2 across the UVC spectrum: KrCl* excimer, mercury-vapor, and light-emitting-diode (LED) sources. Applied and Environmental Microbiology 2021, 87 (22), e01532–01521. [PubMed: 34495736]

(9). Yoshino K; Cheung A-C; Esmond J; Parkinson W; Freeman D; Guberman S; Jenouvrier A; Coquart B; Merienne M Improved absorption cross-sections of oxygen in the wavelength region 205–240 nm of the Herzberg continuum. Planetary and space science 1988, 36 (12), 1469–1475.

(10). Yoshino K; Esmond J; Cheung A-C; Freeman D; Parkinson W High resolution absorption cross sections in the transmission window region of the Schumann-Runge bands and Herzberg continuum of O2. Planetary and Space Science 1992, 40 (2–3), 185–192.

(11). Nicolet M; Peetermans W Atmospheric absorption in the O2 Schumann-Runge band spectral range and photodissociation rates in the stratosphere and mesophere. Planetary and Space Science 1980, 28 (1), 85–103.

(12). Chapman S XXXV. On ozone and atomic oxygen in the upper atmosphere. The London, Edinburgh, and Dublin Philosophical Magazine and Journal of Science 1930, 10 (64), 369–383.

(13). Claus H Ozone generation by ultraviolet lamps. Photochemistry and photobiology 2021, 97 (3), 471–476. [PubMed: 33534912]

(14). Poppendieck D; Hubbard H; Ward M; Weschler C; Corsi R Ozone reactions with indoor materials during building disinfection. Atmospheric Environment 2007, 41 (15), 3166–3176.

(15). Morrison GC; Eftekhari A; Majluf F; Krechmer JE Yields and variability of ozone reaction products from human skin. Environmental Science & Technology 2020, 55 (1), 179–187. [PubMed: 33337871]

(16). Coffaro B; Weisel CP Reactions and Products of Squalene and Ozone: A Review. Environmental Science & Technology 2022, 56 (12), 7396–7411. [PubMed: 35648815]

(17). Peng Z; Miller SL; Jimenez JL Model Evaluation of Secondary Chemistry due to Disinfection of Indoor Air with Germicidal Ultraviolet Lamps. Environmental Science & Technology Letters 2022, 10 (1), 6–13.

(18). Peng Z; Douglas D D; Symonds G; Jenks O; Handschy AV; de Gouw J; Jimenez JL Significant Production of Ozone from Germicidal UV Lights at 222 nm. Medrxiv (preprint) 2023. DOI: 10.1101/2023.05.13.23289946.

(19). Blatchley III ER; Brenner DJ; Claus H; Cowan TE; Linden KG; Liu Y; Mao T; Park S-J; Piper PJ; Simons RM Far UV-C radiation: An emerging tool for pandemic control. Critical Reviews in Environmental Science and Technology 2023, 53 (6), 733–753.

(20). Fukui T; Niikura T; Oda T; Kumabe Y; Ohashi H; Sasaki M; Igarashi T; Kunisada M; Yamano N; Oe K Exploratory clinical trial on the safety and bactericidal effect of 222-nm ultraviolet C irradiation in healthy humans. PLoS One 2020, 15 (8), e0235948. [PubMed: 32785216]

(21). Burkholder J; Sander S; Abbatt J; Barker J; Cappa C; Crounse J; Dibble T; Huie R; Kolb C; Kurylo M Chemical kinetics and photochemical data for use in atmospheric studies; evaluation number 19; Pasadena, CA: Jet Propulsion Laboratory, National Aeronautics and Space …, 2020.

(22). Zhang J-Y; Boyd I; Esrom H UV intensity measurement for a novel 222 nm excimer lamp using chemical actinometer. Applied surface science 1997, 109, 482–486.

(23). Eden S; Barc B; Mason N; Hoffmann S; Nunes Y; Limão-Vieira P Electronic state spectroscopy of C2Cl4. Chemical Physics 2009, 365 (3), 150–157.

(24). Ma B; Burke-Bevis S; Tiefel L; Rosen J; Feeney B; Linden KG Reflection of UVC wavelengths from common materials during surface UV disinfection: Assessment of human UV exposure and ozone generation. Science of The Total Environment 2023, 869, 161848. [PubMed: 36709900]

(25). Barber V; Goss MB; Franco Deloya LJ; LeMar LN; Li Y; Helstrom E; Canagaratna MR; Keutsch FN; Kroll JH Indoor Air Quality Implications of Germicidal 222 nm Light. ChemRxiv (preprint) 2023. DOI: 10.26434/chemrxiv-2023-ft1l8.

(26). Nazaroff WW; Weschler CJ Indoor ozone: Concentrations and influencing factors. Indoor air 2022, 32 (1), e12942. [PubMed: 34609012]

(27). Graeffe F; Luo Y; Guo Y; Ehn M Unwanted Indoor Air Quality Effects from Using Ultraviolet C Lamps for Disinfection. Environmental Science & Technology Letters 2023.

(28). Eadie E; Hiwar W; Fletcher L; Tidswell E; O'Mahoney P; Buonanno M; Welch D; Adamson CS; Brenner DJ; Noakes C Far-UVC (222 nm) efficiently inactivates an airborne pathogen in a room-sized chamber. Scientific reports 2022, 12 (1), 4373. [PubMed: 35322064]

Synopsis

Devices using 222 nm light have potential benefits in virus transmission mitigation. We highlight unintended ozone production from a 222 nm lamp.

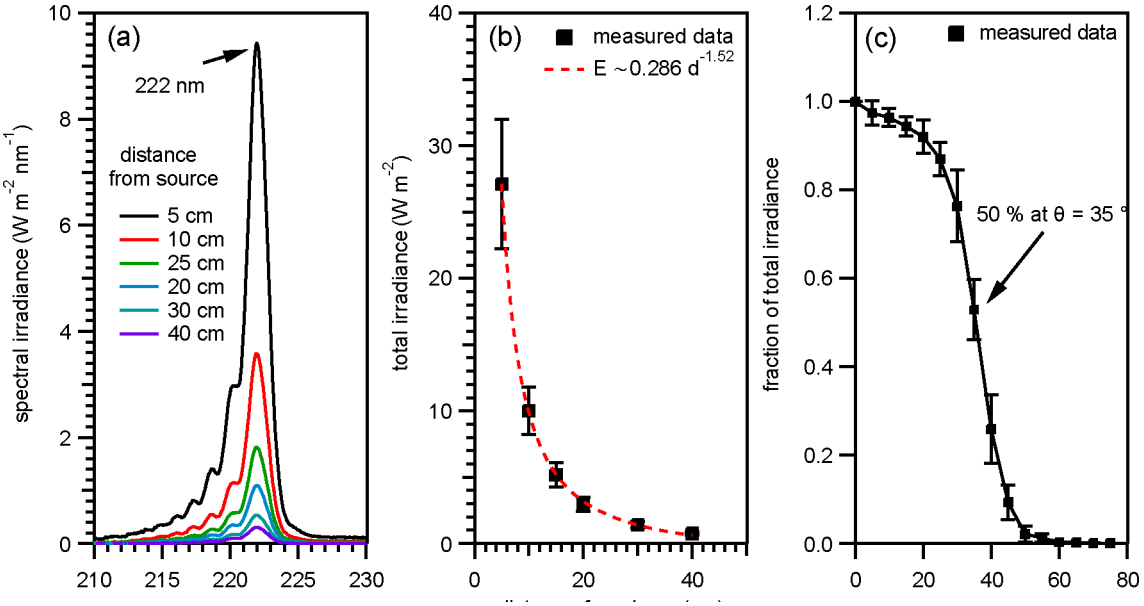

Figure 1.

(a) GUV222 emission spectra measured at six different distances. (b) The total irradiance versus distance. (c) Relative irradiance from GUV222 as a function of projection angle from 0 degrees to 75 degrees.

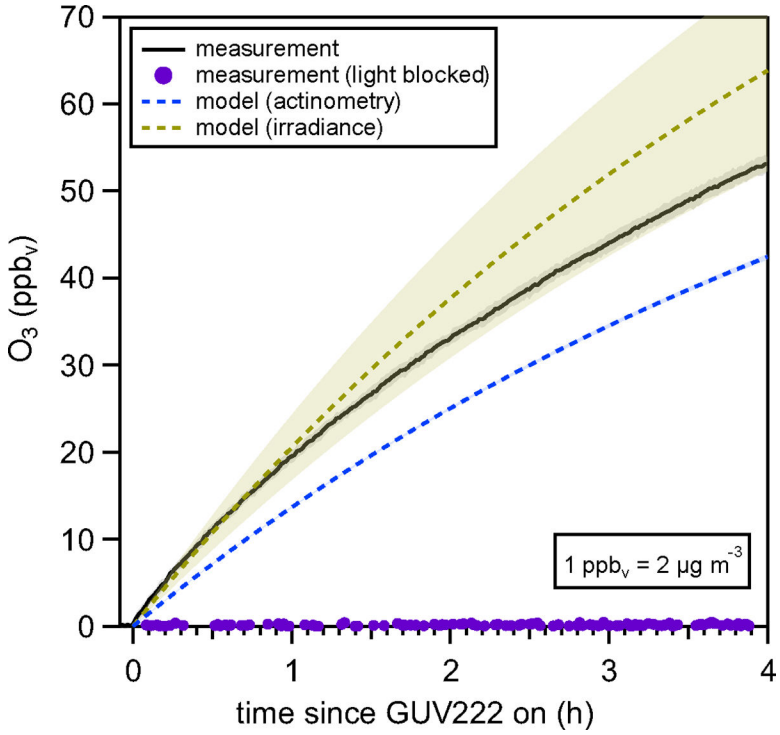

Figure 2.

The average measured O_3 mixing ratio from seven GUV222 experiments is shown as the solid black line with the standard deviation (1σ) shown by the gray shaded area. The average O_3 mixing ratio predicted from the actinometry-informed model is shown as the dashed blue with the variability (1σ) too small to see on this graph. The average modeled O_3, predicted from the irradiance method, is shown in yellow with an 18 % error propagated from the uncertainty in the irradiance measurement. The O_3 measured from the experiment where the light was blocked is shown in purple.

Table 1.

Summary of O_3 decay constants, air change rates ($k_{\dot{V}}$), and O_3 generation rates.

Experiment	k_{decay} (h^{-1})	$k_{\dot{V}}$ (h^{-1})	GR, O_3 generation rate*	
			μg h^{-1}	ppb_v h^{-1}
1	0.172	0.010	1250	19.9
2	0.176	0.014	1220	19.5
3	0.169	0.010	1210	19.3
4	0.168	0.011	1210	19.3
5	0.167	0.012	1200	19.2
6	0.167	0.014	1200	19.2
7	0.171	0.012	1230	19.6
Average (±1σ)	0.170 ± 0.003	0.012 ± 0.002	1220 ± 20	19.4 ± 0.3

*O_3 generation rates will be dependent on GUV222 path length, and thus may vary as a function of the size of a chamber or indoor space. Generation rates were calculated using the measured chamber volume, temperature, and pressure.